

The Brain-Inspired Cooperative Shared Control for Brain-Machine Interface

Shengjie Zheng^{1,2,+}, Ling Liu^{1,2,+}, Junjie Yang^{1,2}, Lang Qian³, Gang Gao^{1,2}, Xin Chen^{1,2}, Wenqi Jin⁴, Chunshan Deng², and Xiaojian Li^{2,*}

¹University of Chinese Academy of Sciences, Beijing, China

²CAS Key Laboratory of Brain Connectome and Manipulation, the Brain Cognition and Brain Disease Institute (BCBDI), Shenzhen Institute of Advanced Technology, Chinese Academy of Sciences; Shenzhen-Hong Kong Institute of Brain Science-Shenzhen Fundamental Research Institutions, Shenzhen, China

³Tsinghua Shenzhen International Graduate School, Tsinghua University, Shenzhen, China

⁴Faculty of Education, Beijing Normal University, Beijing, China

*xj.li@siat.ac.cn

+these authors contributed equally to this work

ABSTRACT

In the practical application of brain-machine interface technology, the problem often faced is the low information content and high noise of the neural signals collected by the electrode and the difficulty of decoding by the decoder, which makes it difficult for the robotic to obtain stable instructions to complete the task. The idea based on the principle of cooperative shared control can be achieved by extracting general motor commands from brain activity, while the fine details of the movement can be hosted to the robot for completion, or the brain can have complete control. This study proposes a brain-machine interface shared control system based on spiking neural networks for robotic arm movement control and wheeled robots wheel speed control and steering, respectively. The former can reliably control the robotic arm to move to the destination position, while the latter controls the wheeled robots for object tracking and map generation. The results show that the shared control based on brain-inspired intelligence can perform some typical tasks in complex environments and positively improve the fluency and ease of use of brain-machine interaction, and also demonstrate the potential of this control method in clinical applications of brain-machine interfaces.

Introduction

The emergence of human-computer interaction has provided an interface for communication between humans and computers, and it is mainly used in service robots to provide convenience to people's lives¹⁻⁷. Due to its low interaction information, the effectiveness of its interaction greatly depends on the intelligence of the robot. However, current developments in the field of robotics are based on simple and controllable working environments and are not as effective when deployed in unstructured and complex environments (e.g., domestic environments) to further advance its development process in applications. Therefore, the low interaction information has led researchers to pursue the possession of embodied intelligence in robots⁸. Embodied intelligence emphasizes the interaction of the system and the environment to solve task bottlenecks in complex environments through the combined capabilities of the brain and the body.

Brain-machine interfaces are advanced forms of human-computer interaction that can be used to read neural signals from the brain and use them as complementary inputs in a human-computer interaction environment to neurologically control various intelligent robots or computer systems⁹⁻¹⁴. It can therefore capture a relatively large amount of information and can better serve paralyzed patients. However, the field of brain-machine interfaces often faces the problem of the low information content of the neural signals collected by the electrodes, high noise, and limited acquisition of brain areas, despite the fact that more data can be obtained by implanting more electrodes, the instability of the information flow leads to the difficulty of the robot to acquire continuous instructions to complete the task^{15,16}. Therefore, the inadequacy of information has also led to the pursuit of intelligent robots by researchers, and how to guide robots to understand complex instructions to assist brain-machine interfaces to accomplish advanced tasks is a great challenge at present.

By means of a brain-machine interface, if the robot interacts with the human brain continuously, it is likely to learn the preferences of how the human brain perceives, reasons, and makes decisions in various complex task scenarios. Such a closed-loop approach that does not rely on a specific environment but communicates with the human brain to build a personalized user preference model and further obtains information from the model for perception and decision-making based on specific tasks is a kind of supervised learning guided by the human brain to obtain human-like reasoning and decision-making capabilities.

And brain-machine interface, as a way of high-bandwidth human-robot interaction, can help humans to better utilize their brain and body potential. By intelligently fusing the human brain with the robot and combining fuzzy abstract-level commands with concretely executed control commands to achieve mindfulness, a high-performance brain-machine interface is achieved to help people accomplish a series of complex tasks.

Robots with brain-computer intelligence integration solutions can make fast decisions based on user preference models in various task scenarios, and the user preference models will gradually approximate the real picture of the user as the number of brain-machine interactions increases. In this scheme, only a small amount of neural information is required to make the brain-machine interface work well. Thus, it can use low information to allow the robot to serve humans effectively, and conversely, humans learn by supervising the robot so that it can be endowed with human-like cognitive and decision-making abilities to reach the level of intelligence control.

In most cases, clinical brain-machine interface applications require collaborative control algorithms^{17,18}. This is because the sensorimotor areas are not the only building blocks of behavioral control, but also the cerebellum, brainstem, and spinal cord are jointly involved. For example, when a person is about to fall and instinctively controls the stability of the body, this behavior is not controlled by brain thinking and then decision making; such a consistent behavior is a solid action pattern acquired through long-term repetitive learning¹⁹. It has also been shown at the level of mathematical abstraction that the primary motor cortex performs a regression task, decoding finely controlled motor trajectories, while the secondary motor cortex decodes abstractly controlled motor intentions, a categorization task²⁰. The underlying dynamics of cortical sensorimotor areas are stable when monkeys are allowed to learn a fixed brain control task repeatedly. Combined with the consistency characteristics of the movement modality, this paper proposes an efficient scheme for brain-controlled intelligent robots using a collaborative shared control strategy. Once the monkey learns this motor control task, it can perform the behavior quickly and precisely.

Brain-controlled intelligent robots can provide monkeys with "precise control" and "dual-purpose" skills by using a rule-based finite state machine method, which is a discrete mathematical model consisting of four elements: state, transfer, event, and action. By establishing a behavior rule base based on the current task route and environment, and making behavior decisions for different states, the brain-controlled robot can be provided with multi-state adaptive capabilities.

Taking the behavioral decision based on the monkey grasping food during motion as an example, it is mainly divided into the motion top-level state machine and the sub-state machine under the predation top-level state machine, and the sub-state machines include stopping preparation, stopping, fast food grasping, fine-control grasping, and carriage keeping motion. The predation sub-state machine is set under the predation top-level state machine to model the logic of robotic arm grasping in different wheeled robots-driving states during predation. The predation behavior decision is similar to that of humans grasping food, when the monkey sees the food, it controls autonomously whether to grasp and whether to stop. Two modes of fast grasping and fine control are set for grasping food. When there is only one serving of food, the monkey directly takes fast grasping and delegates the task to the robotic arm to complete; when there are multiple servings of food, the monkey can take fine control mode, when the robotic arm moves quickly to the multiple targets, after which the control switches to itself and the monkey controls the fine details of grasping autonomously. This collaborative shared control strategy is important for BMI, which provides an effective window for multitasking parallelizability processing, and the intelligent switching of control reduces the risk of accidents and unnecessary user control difficulties during control while maintaining the ability of the intelligent robot to continuously learn.

Repeated execution of such typical tasks is a continuous teach-commission process and migration of information and workload. Although many laboratories are investigating ways to improve decoder performance to provide patients with more flexible degrees of freedom and more stable manipulation, the amount of information available to the decoder decreases over time, requiring constant recalibration to restore its functionality, and recalibration imposes an additional cognitive burden on the user²¹. Therefore, the scheme in this paper applies brain-inspired intelligence to robots to assist subjects in collaborative shared control, providing a reliable path for users to perform complex tasks.

The flexibility of a brain-controlled intelligent robot needs to rely on efficient software and hardware assistance, and its core functional modules are the perception module, decision module, and control module. The perception module determines the next action to be performed (wheeled robots movement, robotic arm movement, etc.) by obtaining the decoding information from the decoder, and obtaining the target location and the map information of the current space based on the sensing information from the on-board camera; the decision module constructs the decision space and plans the desired motion path based on the information provided by the perception module; the control module controls the wheeled robots or robotic arm to track the desired trajectory based on the desired trajectory given by the decision module. The control module controls the wheeled robots or robotic arm to track the desired trajectory according to the desired trajectory given by the decision module. In the perception module, a convolutional neural network (CNN) network is used to build a visual recognition system, specifically, YOLOv5 is used to achieve target detection, which can be used as technical support for embedded wearable devices due to its lightweight and high accuracy characteristics, in line with the efficiency of brain-controlled robots. In the control

module, a spiking neural network (SNN) is used to build the motion control system, which is more robust compared to artificial neural networks (ANN) and can better cope with the changing and complex environment, in line with the intelligence of brain-controlled robots.

This spiking neural network (SNN) based on brain-inspired intelligence has remarkable bio-interpretation as well as robustness for brain-machine interface tasks and neuroscience research. SNN can be used as a novel control algorithm to provide assistance after the decoder has deciphered the user's intent. In this way, this shared control can be more stable and efficient as it allows for more precise motor control during the execution of high-precision tasks while allowing the subject to have direct control over the vast majority of the movements. We designed offline experiments to validate our system, with macaques as experimental subjects participating in our task. The experimental results show that the use of a brain-computer intelligence integration scheme can efficiently assist in typical tasks in complex scenarios and that a collaborative shared control system can effectively assist in brain-machine interface tasks, making BMI more useful to us in a wide range of scenarios.

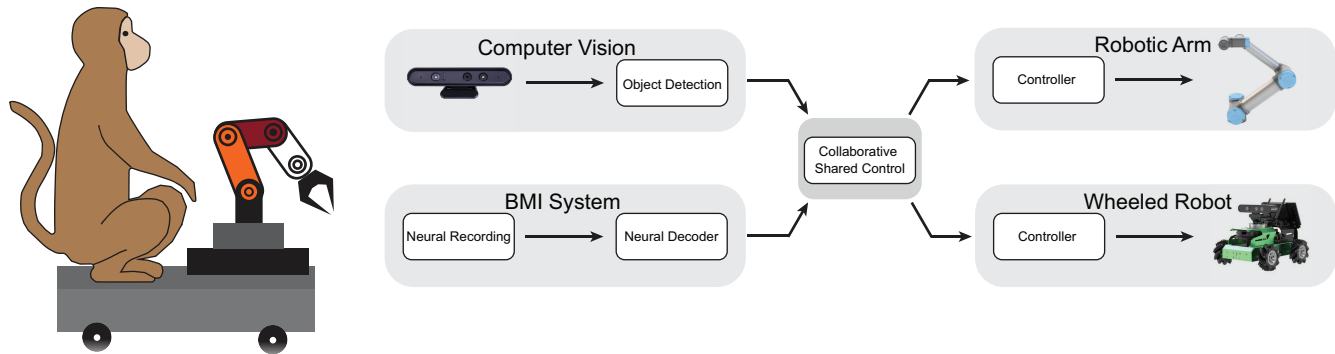


Figure 1. Brain-machine interface cooperative shared control system

Methods

In this section, we present the shared control strategies for the robotic movement, respectively for different tasks that assist the brain-machine interface: grasping control of the robotic arm and control of the speed and direction of the wheel. Firstly, we discuss the computer vision algorithm that provides object detection for the control task and the camera calibration and coordinate transformation involved. Secondly, we discuss the robotic arm grasping system. Lastly, we discuss wheel speed control and orientation encoding algorithms.

System specification

The proposed brain-inspired shared control system mainly has a computer vision subsystem, a robotic arm for motion control based on spiking neural networks, and a mobile wheeled robots implemented based on spiking neural networks. Computer vision provides the function of object detection, while the SNN-based motion control algorithm moves the robotic arm from the initial position to the vicinity of the target. After grasping the target object, the object is moved to a predefined area. In addition, the SNN-based motion control algorithm enables the wheeled robots to efficiently move toward the target location and can track the target and generate a dense semantic map. Fig. 1 shows the schematic diagram of the proposed system.

Computer vision system

The computer vision system uses the YOLOv5 algorithm for object detection, which has a good speed-accuracy balance, especially for its excellent computational speed. Next, a camera is used for acquiring RGB images of the working area. The camera is placed at a fixed position outside the robotic arm and above the mobile wheeled robots and is calibrated by using Zhang method²² to obtain the internal and external reference matrix, distortion model coefficients, and correction matrix of the camera.

For the target recognition module of the robotic arm, using binocular cameras, the target object's image coordinates in the left and right cameras can be obtained through the target recognition algorithm based on YOLOv5s. The coordinate conversion module randomly initializes the world coordinates when the image coordinates of the target object in the left and right cameras are known, and uses Newton's method²³ to continuously approximate the real-world coordinates based on the coordinate conversion formula to pass the world coordinates to the robotic arm control module, so that the robotic arm can move to the target object position for grasping.

For the target recognition module of the mobile wheeled robots, the camera is Orbbec Astra Pro, which comes with a depth camera for 3D reconstruction, SLAM, etc. The object detection module detects the target information and gets the depth image

information from the camera, while the mobile wheeled robots controls the steering based on the distance between the target boundary information and the center point of the screen, and controls the forward and backward based on the target distance information.

We choose the YOLOv5s algorithm as the object detection algorithm due to the fact that YOLOv5s can achieve better results with less resource consumption. The training process requires data augmentation on different datasets, then testing the detection speed and detection accuracy of the algorithm, and finally analyzing and selecting the model to suit the inference of low computing power computing platforms, The system framework as shown in Fig. 2.

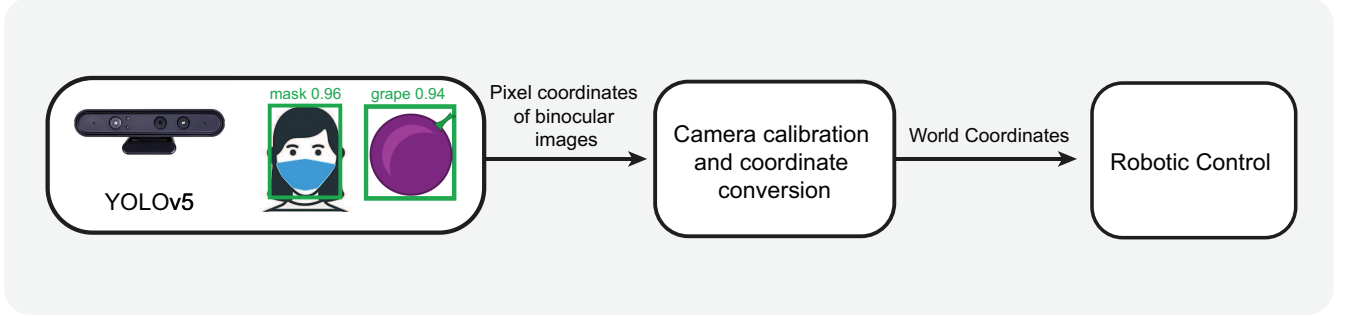


Figure 2. The computer vision system framework.

Robotic arm grasping system

We use the adaptive robotic arm control model proposed by Travis et al²⁴. It is called the recurrent error-driven adaptive control hierarchy (REACH) Model, as shown in Fig. 3. it is a motion control method based on spiking neural networks and has extremely strong biological properties for robotic control. To some extent, the network structure of the model can reproduce the properties associated with real biological motor control. The control model of the robotic arm is shown in the equation 1.

$$M(q)\dot{q} + C(q, \dot{q}) + G(q) + U_{\text{adapt}} = U \quad (1)$$

where, q denotes the coordinates of each joint of the robotic arm, \dot{q} denotes the angular velocity of each joint of the robotic arm, $M(q)$ denotes the inertial force on each joint caused by the acceleration of the motion of each joint of the robotic arm, $C(q, \dot{q})$ denotes the inertial force on the other joints caused by the velocity of the motion of each joint of the robotic arm, i.e., the Coriolis force or centrifugal force, and $G(q)$ denotes the gravitational force of the robotic arm itself to be overcome by each joint of the robotic arm. U_{adapt} denotes our adaptive correction signal (correction torque) calculated by our adaptive regulator. U denotes the required torque applied to each joint actuator according to the robotic arm control model we build to make the joints move according to the specified trajectory (position, velocity, acceleration).

In the dynamics model of the robotic arm control, U_{adapt} denotes the correction signal (correction torque) calculated by our adaptive regulator, and this correction torque is learned by the spiking neural network.

$$\begin{aligned} U_{\text{adapt}} &= Y_d(q)\theta_d \\ M(q)\ddot{q}_d + C(q, \dot{q})\dot{q}_d + G(q) &= Y_d \end{aligned} \quad (2)$$

where $Y_d \in R_{n \times d}$ is the set of basis functions, $\theta_d \in R_{d \times 1}$ is the learning parameter, where n is the number of basis functions, and d is the dimensionality of the control signal U .

$$\theta_d = L_d X_d \otimes ((\dot{q} - \dot{q}_{\text{des}}) + \Lambda(q - q_{\text{des}})) \quad (3)$$

L_d is the learning rate, $X_d \in R_{1 \times n}$ is the basis function in vector form, q and q_{des} are the current and target joint angles, \dot{q} and \dot{q}_{des} are the current and target joint velocities, \otimes is the outer product operation, and Λ is a symmetric positive definite matrix.

The spiking neural network is built based on the Neural Network Engineering Framework (NEF), using the currently generated control torque U as the training signal, the current desired joint angle q_{des} and angular velocity \dot{q}_{des} of the robotic arm as the learning signal, and the learning rule PES (Prescribed Error Sensitivity) as the rule for updating weights in the

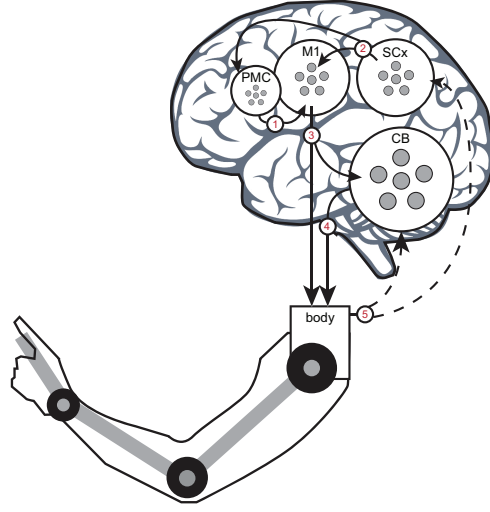


Figure 3. An overview of the REACH model²⁴, shown controlling a three-link arm. Numbers identify major communication pathways. Dashed lines indicate closed-loop feedback signals generated from the senses. The image modified from Travis et al²⁴.

spiking neural network. Also, the neuron type is specified as Leaky Integrate and Fire model (LIF), and the number of neurons is 1000. The activity of neurons inside this spiking neural network can be expressed as the equation 4.

$$a = G[\alpha e \cdot \mathbf{x}] \quad (4)$$

Where $G[\cdot]$ is the nonlinear neural activation function, determined by the specific neuron model. Where a is the activity representation of the neuron, α is the scaling factor (gain) associated with the neuron, e is the neuron's encoder, and \mathbf{x} is the vector to be encoded which is the input data.

The decoded estimate is the sum of the activity of each neuron, weighted by the n -dimensional decoder.

$$\bar{x} = d \otimes a_k \quad (5)$$

where d is the decoder and a_k is the activity of the neuron. The decoder is found by minimizing the difference between the decoding estimate and the actual coding vector by least squares estimation. The neuron decoder d is calculated as the equation 6.

$$\mathbf{d} = \Upsilon^{-1} \Gamma \quad \Gamma_{ij} = \int a_i a_j dx \quad \Upsilon_j = \int a_j \mathbf{x} dx \quad (6)$$

In equation 6, $a_i a_j$ is the respective signal activity of neuron i and neuron j , and \mathbf{x} is the input data. We used a supervised learning rule based on Prescribed Error Sensitivity (PES) for training spiking neural networks.

$$\begin{aligned} \Delta \mathbf{d}_i &= \kappa \mathbf{E} a_i \\ \Delta \omega_{ij} &= \kappa \alpha_j e_j \cdot \mathbf{E} a_i \end{aligned} \quad (7)$$

where κ is the scalar learning rate, \mathbf{E} expressed as the error vector by minimizing expectations, \mathbf{d} denotes the decoder, and ω denotes the connection weights, and the other terms are the same as the above equation. The PES rule enables the spiking neural network to minimize the error signal while allowing the network to learn to compute the transformation online.

The connection weight between neuron i and neuron j is calculated as the equation 8:

$$\omega_{ij} = \alpha_j e_j \mathbf{d}_i \quad (8)$$

where a_j is the scale factor (gain) of neuron j , e_j is the encoder of neuron j , and \mathbf{d}_i is the decoder of neuron i .

$$a \omega \otimes d = U_{adapt} \quad (9)$$

where a is the activity of neurons, encoded from the input data, ω is the connection weight between neurons, d is the neuron decoder, and U_{adapt} is the final output correction torque. Finally, the whole robotic arm control framework is shown in Fig. 4.

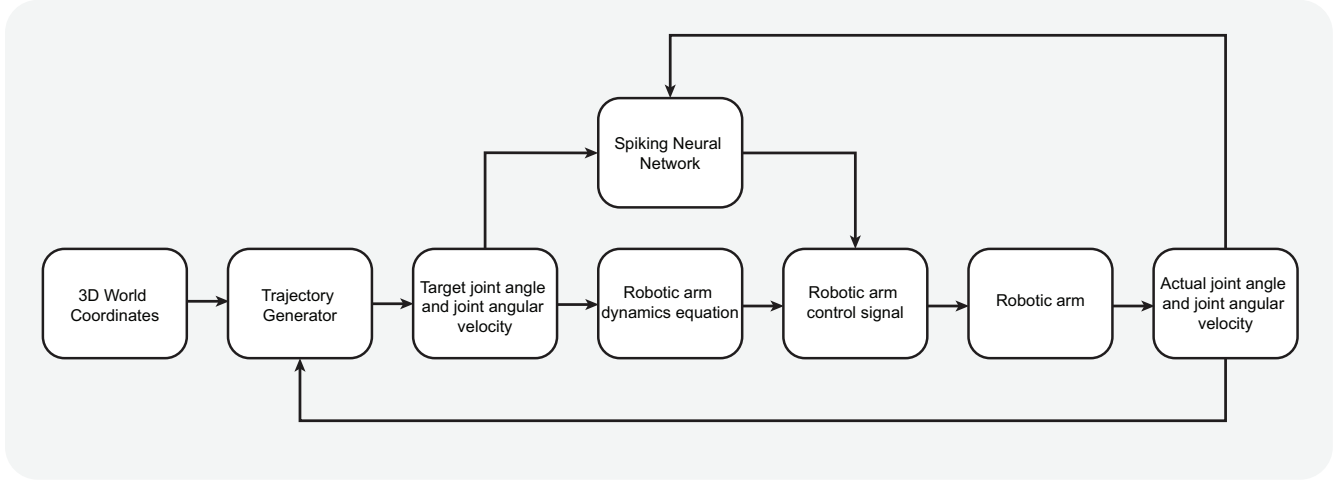


Figure 4. The robotic arm control flow

Wheel speed control

In current mobile robots, differential drive is still the mainstream. The use of differential drive method for control will result in the wheeled robots not being able to "go straight" stably. Due to the limitation of the preparation process, the drive characteristics of the motors controlling the two wheels themselves cannot be identical, the shape and size of the two motors cannot be exactly the same, and the precision of the assembly will also be different; the wheels may slip or encounter small obstacles when rolling during the driving process. All of these will cause the speed of the left and right wheels to be different and thus not go straight.

The open-loop control without feedback mechanism cannot eliminate the speed error of the above left and right wheels because the above disturbance is random. In order to make the wheeled robots go in a straight line, the only way is to realize closed-loop control, so that when the wheeled robots is disturbed, feedback can be given to the left and right wheels in time to correct the speed deviation of the two wheels, then the wheeled robots can go in a straight line.

In the field of mobile robotics, the combination of PID algorithm and wheel speed detection device is a common method to solve the problem of "not going straight", but it is not suitable for complex environments and cumbersome to adjust the parameters, and the wheel speed detection device is not necessarily suitable for the off-the-shelf wheeled robots motor solution.

Spiking neural network has the characteristics of low power consumption and good dynamics. Spiking neural networks can combine Inertial Measurement Units (IMUs) to provide a highly adaptive, relatively low-power solution to the problem of "not walking straight".

Pulse Width Modulation (PWM) is generally used for wheeled robots wheel speed control. The PWM adjusts the analog circuit primarily through the digital output of the microprocessor, which equates the desired waveform by modulating the width of the pulse to control the speed of the wheeled robots. The overall control flow is shown in Fig. 5.

Control state processor: Since the value of PWM varies with the required speed of wheeled robots each time, in order to adapt the PWM value to the neuron model of the spiking neural network, the value needs to be scaled, and there can be various options for the specific scaling method, the common rescaling is shown here, and the idea is to map the PWM value linearly to the interval $[0, 1]$ with the following equation 10.

$$x' = \frac{x - \min(x)}{\max(x) - \min(x)} \quad (10)$$

Angle processor: The similarity between angle processing and PWM processing is that both of them use rescaling method in order to adapt to the neuron model of multiple spiking neural networks. The difference is that PWM is mapped to the interval $[0, 1]$ while angle is mapped to the interval $[-1, 1]$, and the positive and negative values of angle are used to represent the offset direction of the wheeled robots, which is given by the following equation 11.

$$\theta' = \frac{\theta - \text{mean}(\theta)}{\max(\theta) - \min(\theta)} \quad (11)$$

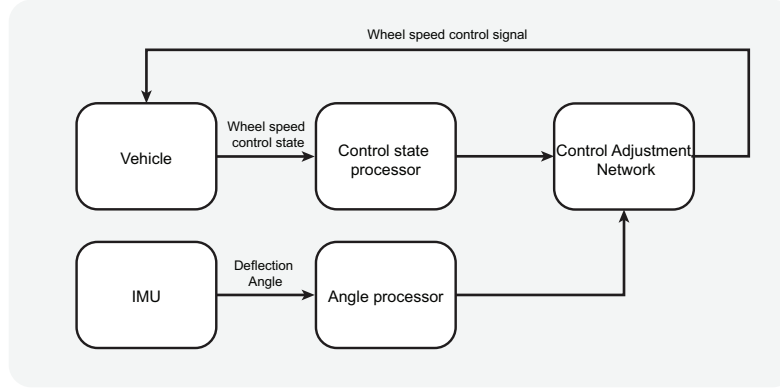


Figure 5. The wheeled robots control flow.

Control adjustment network: this part is implemented by the spiking neural network, this network accepts the PWM control signal output by the control state processor as the training signal and the angle signal output by the angle processor as the learning signal, and uses the corresponding SNN to tune the control signal using supervised learning algorithm.

There are various supervised learning algorithms that can be replaced according to the needs. Here we show the PES (Prescribed Error Sensitivity)²⁵ supervised learning algorithm and its homeostatic Prescribed Error Sensitivity (hPES)²⁶ algorithm combined with the unsupervised learning algorithm BCM(Bienenstock, Cooper, Munro).Where the PES learning rule is shown in equation 12.

The weights of the unsupervised algorithm BCM are the following equation 12.

$$\Delta\omega_{ij} = a_i a_j (a_j - \varepsilon) \quad (12)$$

Where ε is modification threshold. The hPES weight update formula is obtained according to equation 8 and equation 12, as shown in equation 13.

$$\Delta\omega_{ij} = \kappa \alpha_j a_i (S e_j \cdot \mathbf{E} + (1 - S) a_j (a_j - \varepsilon)) \quad (13)$$

Where S is the relative weighted value of the supervised part and the unsupervised part. The \mathbf{E} can denote the angular information θ' .

Directional coding based on spiking neural network

Continuous attractor neural network (CANN) is a network computational model with some generality for the brain to encode, store, compute and communicate information²⁷. The application of continuous attractor neural networks for modeling neural information processing has started early, and classical successful examples include head orientation coding²⁸, spatial location coding²⁹ etc. These works also show the importance of continuous attractor networks. Biological evidence for the real existence of continuous attractor networks has also emerged frequently in recent years. For example, head-oriented neurons were observed in the Drosophila brain to be spatially distributed along a ring like the model of the continuous attractor network, and the neuronal population activity followed the smooth rotation together with the drosophila head rotation³⁰.

In head orientation coding, head orientation neurons within the brain form a one-dimensional continuous attractor network through interaction connections. The activity of the neuron population of the network forms a wave packet in real time, and its vertex position encodes the head orientation information; using the feature that the interaction between neurons of the continuous attractor network has translational invariance, a wheeled robots orientation control model with the continuous attractor network as the main body is constructed to respond to the brain's encoding process of continuous variables such as orientation and motion direction. The equation of the continuous attractor network is as the following equations 14.

$$\begin{aligned} \tau \frac{dU_c}{dt} &= -U_c + \rho \int_{c'} J_{c,c'} \gamma_{c'} dc' + I_c^{ext} \\ \gamma_c &= \frac{U_c^2}{1 + k\rho \int_{c'} U_{c'}^2 dc'} \\ J_{c,c'} &= \frac{J}{\sqrt{2\pi a}} e^{-\frac{(c-c')^2}{2a^2}} \end{aligned} \quad (14)$$

where c denotes a set of neurons encoding a one-dimensional continuous stimulus, ρ denotes neuronal density, and τ is the time constant of neurons. U_c denotes the average input to a cluster of neurons. I_c^{ext} denotes an external stimulus. γ_c denotes the firing rate of c . Equation 14 in which k is a positive constant to adjust the degree of inhibitory connectivity. $J_{c,c'}$ denotes the interaction between neuronal clusters c and c' , and J denotes the magnitude of the interaction.

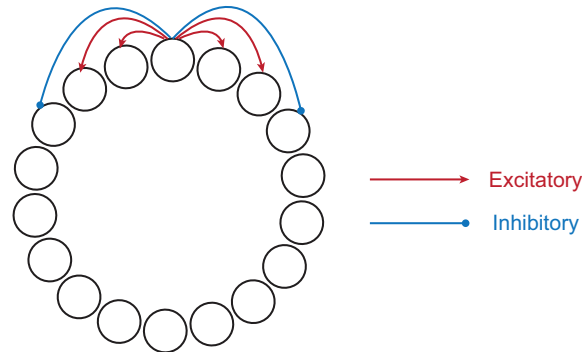


Figure 6. The structure of attractor network, a network of nodes, often recurrently connected, whose time dynamics settle to a stable pattern.

Experiment

Object detection

We use the YOLO algorithm to implement object detection for the robotic arm and wheeled robots tasks. Among them, the object detection in the robotic arm grasping project uses the Grape dataset.

The object detection in the wheeled robots task uses the Masked Face dataset as the test set³¹, which includes a large number of images of face masks in addition to the normal images with and without masks. A series of data enhancement methods were used in the experiments, including random cropping, horizontal flipping, random contrast adjustment, adding Gaussian noise, and random brightness adjustment. After data enhancement of the dataset, the dataset was randomly disrupted and set the ratio of the training set to the test set to 9:1.

Robustness experiments are designed for the recognition of the target object, and the robustness of object detection in pictures is experimented with from five aspects of brightness, occlusion, rotation, stretching, and noise, as shown in Fig. 7.

The Masked Face and Grape dataset is detected and recognized, and from Fig. 7. It can be seen that the model can effectively recognize Masked Face and Grapes, and the model has some robustness.

Robotic arm movement control experiments

For robotic arm grasping control with the brain-machine interface, we based on the work of Travis et al²⁴, build a UR5 robotic arm simulation model on the simulation software CoppeliaSim, and control the simulated robotic arm using an spiking neural network based on the Nengo framework³², thus implementing the spiking neural network based robotic arm control algorithm as well as performance testing, the robotic control framework is shown in Fig. 8.

The UR5 model consists of six joints and six connecting rods. Among them, the two most critical joints with the largest range of motion are joint1 and joint2, as shown in Fig. 9.

An identical force is applied to the six joints of the arm during the motion of the arm to simulate a real-world scenario. This unexpected force is set to 1/8 of the robot arm's own gravity. The two joints joint1 and joint2 with the largest range of motion in the UR5 robot arm are selected, and the end position of the UR5 robot arm is taken as the starting position, and the four ending positions are selected, i.e. the distance $(\Delta X, \Delta Y, \Delta Z)$ between their target positions and the starting position, which are $(0.2, 0.2, 0)$, $(0.2, -0.2, 0)$, $(-0.2, 0.2, 0)$, $(-0.2, -0.2, 0)$ respectively.

The conventional PID control algorithm and the spiking neural network-based robotic arm control algorithm are used to control joint1 and joint2 respectively, comparing the arc variation from the start to the target position and the distance variation between the start position and the target position.

In the case of $(\Delta X, \Delta Y, \Delta Z) = (\pm 0.2, \pm 0.2, 0)$, there are four different directions of the termination position, respectively, under the control of the SNN-based robotic arm control algorithm and PID (Proportion Integral Differentia) control algorithm, 20 simulations were done in each of the four different directions, from which one was selected each time, for a total of eight times, to plot the change in radian of the two joints (joint1 and joint2) of the simulated UR5 robot arm from the starting position to the target position, and also the change in distance between the starting position and the target position.

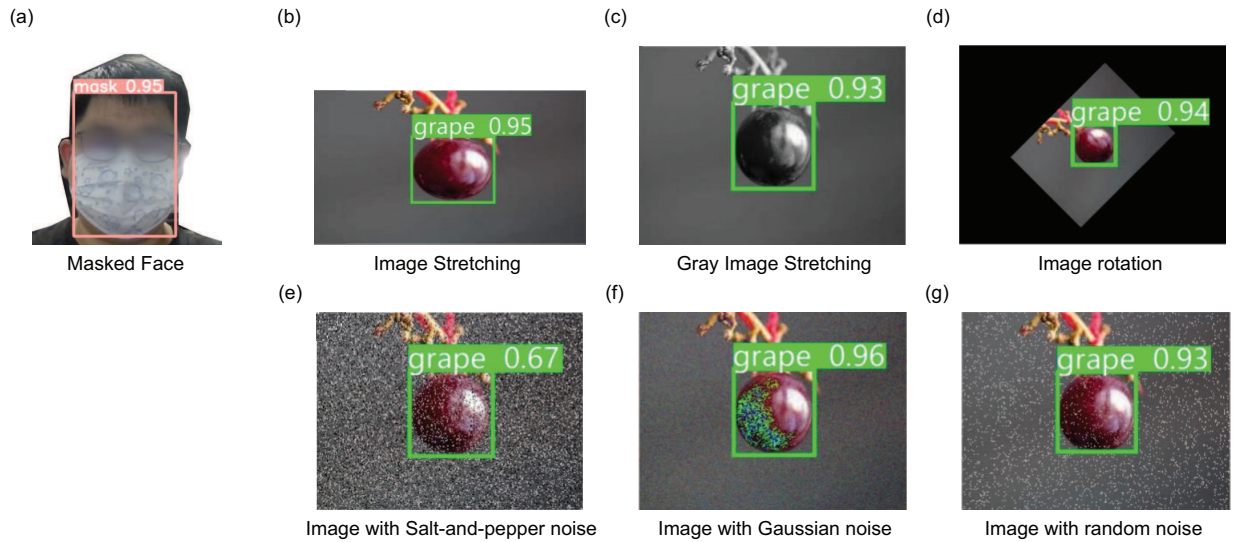


Figure 7. The object detection based on YOLOv5s.

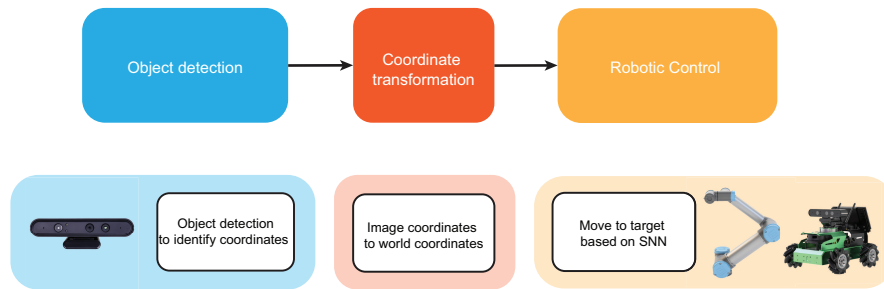


Figure 8. The overall framework of the control system.

Wheeled robots speed control and direction orientation experiment

For wheeled robots movement control with a brain-machine interface, we use Robot Operating System (ROS) to combine the wheel speed and direction control module and target detection module for wheeled robots vision tasks. After the camera detects an unmasked object by the object detection module, it will use the spiking neural network control module to move in the direction of the object. The system's object detection module is connected to the SNN module through ROS distributed communication.

The experiments were conducted using a Raspberry Pi-based two-wheeled circular wheeled robots, which uses two N20 motors to drive the two wheels separately. An Inertial Measurement Unit (IMU) was added on top of the cart to monitor the cart's heading angle in real-time. Using the Nengo³² framework to build SNN for wheel speed control, and homeostatic Prescribed Error Sensitivity (hPES) supervised learning rules are used to detect the heading angle and regulate the left and right wheel speeds in real-time.

The wheeled robots wheel speed control experiment was conducted on uneven ground, and after several tests, the final test results are shown in Fig. 10. After the adjustment of the wheel speed adaptive network, the directional deflection problem of the wheeled robots is controlled, and the angular deflection is slightly oscillating around 0 degrees, and the effect is similar to that of the classical PID algorithm. It proves that the network has a certain deflection correction capability.

We used the attractor network to encode the orientation information of the moving wheeled robots. The attractor network is implemented with reference to Si Wu et al for the design and parameter configuration of the attractor network²⁷. For testing, 360 neurons were used, each with excitatory connections to its left and right 90 neurons, as shown in Fig. 6, with each neuron responding to the direction as shown in Fig. 15.

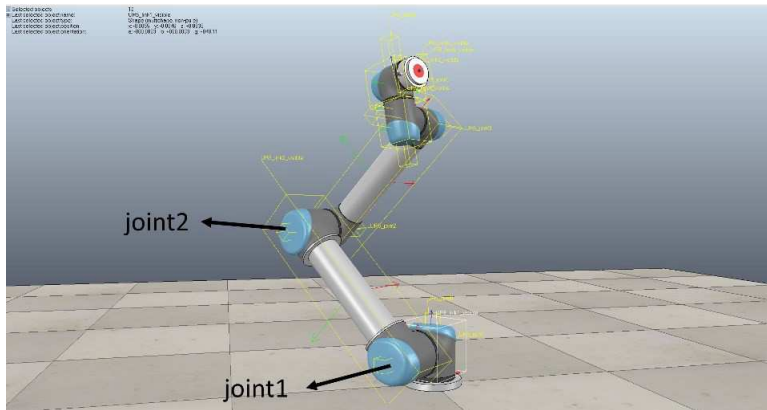


Figure 9. The UR5 robotic arm runs on the simulation software CoppeliaSim.

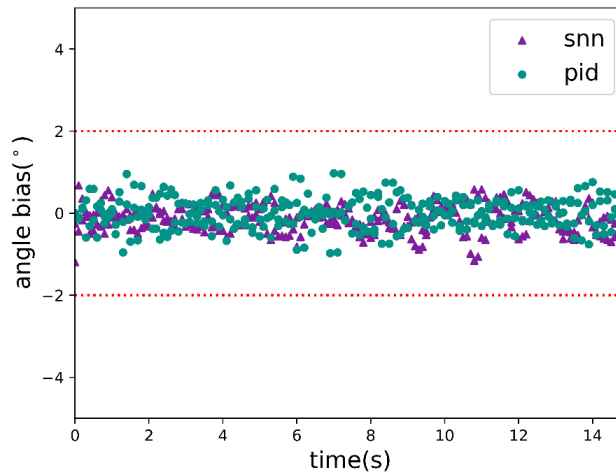


Figure 10. Comparison of wheel speed regulation with different algorithms.

Results

In the case study under consideration, we want the robot can perform different functions based on discrete instructions with a certain degree of accuracy and robustness. Robots can also be executed more efficiently than traditional algorithms. In the following, we discuss the experimental results for different robots.

Robotic arm movement control

In order to test the immunity performance of the robotic arm to the external environment under the control of the Proportional–Integral–Derivative (PID) algorithm and SNN-based robotic arm control algorithm, respectively. During the motion of the arm, an identical force is applied to the six joints of the arm to simulate a real-world accidental disturbance situation. The accidental force cannot be set too large to prevent the arm from moving, nor too small to interfere with the arm’s motion, and after several tests, the range is roughly between 1/4 and 1/16 of the arm’s own gravity. time. When the robotic arm is stabilized, the square of the distance from the target position is recorded, as shown in the Figure 11 and 12.

From the simulation experiment results, it can be seen that the robotic arm moves to different termination positions in four directions and unexpected force is applied to the robotic arm. It can be seen that the spiking neural network control algorithm can control the robotic arm to approach the target position faster than the PID algorithm, and the time is more than 10% faster. Also, when the robotic arm is stabilized, the square of the distance from the target position is recorded, and it can be seen that the spiking neural network control algorithm can control the robotic arm closer to the target position compared to the PID control algorithm, compared to just the accuracy is not obvious.

Therefore, during the movement of the robotic arm, when there is unexpected interference, the spiking neural network

control algorithm can control the robotic arm to approach the target position faster than the traditional PID control algorithm, which can better assist the brain-machine interface task.

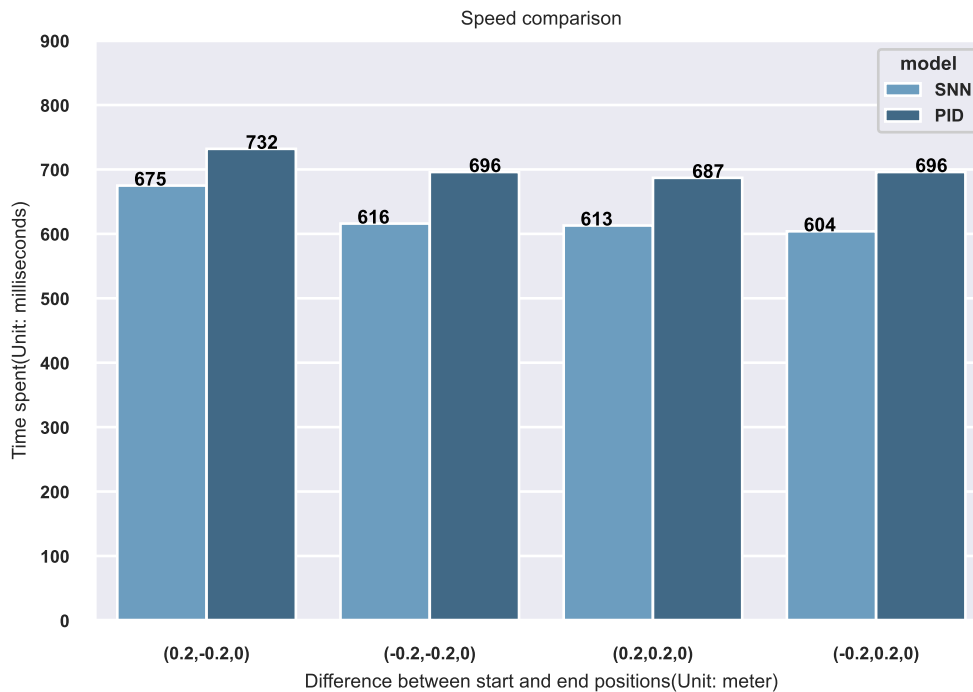


Figure 11. Comparison of robotic arm movement speed with different algorithms.

Wheeled robots Object Tracking

We deploy the spiking neural network control module and the object detection module on the wheeled robots and the laptop, respectively, and perform target tracking tests, as shown in Fig. 13 shown. When the set object appears within the range of the wheeled robots camera, the wheeled robots will follow the object. When the object moves backward and forward, the wheeled robots will also move backward and forward at the same time. The experiment proves that the spiking neural network control module and the object detection module have been successfully combined and are able to perform the task as a mobile robot.

Using common Simultaneous localization and mapping (SLAM) algorithms for simultaneous map construction during the tracking process can provide complete map information and expand the usage scenarios of the system. The experiments use the open source gmapping³³ in Robot Operating System (ROS) for map generation, and after letting the experimental wheeled robots follow the experimenter around the room, the final result is shown in Fig. 14. The results show that the map can provide rich semantic information, and object detection is also relevant for the optimization of map accuracy and the construction of semantic maps.

In our experiments, we tested the directional encoding of the wheeled robots by feeding additional Gaussian noise involving all neuron positions to the steady state of the attractor network. The results show that the attractor network can still maintain a relatively stable state for a certain period of time, as shown in Fig. 16 is shown. The attractor network can maintain a relatively stable firing state even after receiving these anomalous inputs, which shows the high robustness of the attractor network against random noise, constant bias and extreme outlier inputs.

According to the above properties of the continuous attractor network, it is very similar to the navigation characteristics of animals represented by a navigation-related cellular encoding. The spiking neural network can assist mobile wheeled robots and robots with advanced tasks such as spatial cognition, memory, and navigation and is extremely bio-interpretable. Therefore, sending real-time detected object information to the spiking neural network control module for motion control of the experimental wheeled robots can fully utilize the advantages of spiking neural networks for directional movement.

Prospects and Challenges

In this proof-of-concept study, we demonstrate how brain-inspired intelligence can be applied to brain-machine interface shared control tasks by combining a BMI system with vision-guided robot control to improve robotic arm mobile grasping and

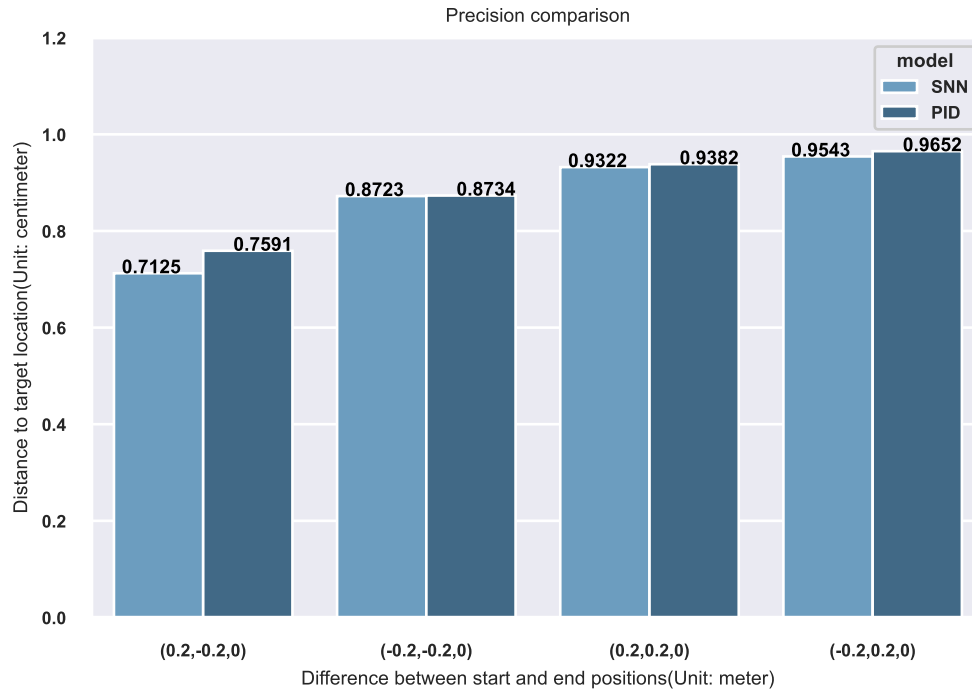


Figure 12. Comparison of robotic arm movement precision with different algorithms.

wheel speed orientation tasks for mobile wheeled robots. Once the computer vision recognizes the objects in the workspace, the brain-inspired intelligence-based shared control algorithm can implement complex tasks based on the intent of the BMI. Our goal is to maintain as much consciousness-based control as possible while assisting the most difficult parts of the task. When the shared control system detects the user's motion intent, BMI's robots will perform the corresponding task. The ultimate goal is adjustable autonomy, using any available BMI signal for maximum effectiveness.

Several published experiments on shared control systems involving BMI, such as Handelman et al.³⁴. They proposed a collaborative shared control strategy to manipulate and coordinate two modular prosthetic limbs (MPLs) to perform a two-handed self-feeding task and achieved considerable accuracy. The classifier can distinguish multiple gestures. However, multiple shared control parameters in the system require manual adjustment and cannot yet be automatically calibrated and extended to other tasks. In a study by Dunlap et al.³⁵, steering and speed control were achieved by accurately encoding motor intent from the participant's motor cortex and translating the intent into wheeled robots control commands. This is then a conceptual work because, in reality, driving a wheelchair or a wheeled robots is a complex task that poses many risks and serious consequences if a malfunction occurs. The controller for the brain-machine interface must have adequate response time, fault tolerance, and fault mitigation methods. Therefore, current shared control systems for BMI work well for specific tasks, but they cannot yet be extended to real-world use.

Our approach uses a BMI-based shared control system for offline experiments to achieve robotic arm movement control and mobile wheeled robots movement direction tasks. In our shared control strategy, the robotic system can achieve better performance. The SNN-based control algorithm shows excellent robustness to external forces and noise. Thus, this approach provides us with a better understanding of the expected achievable performance of the robotic arm motion control.

Shared control based on brain-inspired intelligence algorithms is a forward-looking attempt that can be extended to different brain-machine interface tasks. However, there are still many challenges. Such as degraded signal quality or limited neural information that can be recorded, making the control effect more limited for the subjects. In this approach, the spiking neural network has not yet shown significant superiority over artificial neural networks in specific tasks. Compared to simulation, using BMI for robotic arm mobile grasping and wheeled robots navigation in real life poses additional challenges. For example, the range of control of the robot and the planned path may significantly affect the subject's fine control of specific movements. Moreover, the vast majority of current BMI tasks are based exclusively on visual feedback, which may lead to ineffective and unstable grasping^{36,37}. This may require further optimization to improve the robot for more bio-interpretable adaptive control. Future work might investigate whether spiking neural networks can simulate biological motor control circuits, especially the motor conduction pathways between the cerebellum, brainstem, and spinal cord, allowing spiking neural networks to act as



Figure 13. The wheeled robot is tracked with Masked-Face as the target. (a), (c) are the images taken by the camera. (b), (d) are wheeled robot for target tracking.

extensions of biological neural networks.

With the development of integrated circuits and material science, BMI can be easily portable, but the current BMI experiments are still limited to the laboratory and have not been able to be used as a medical aid for outdoor use. At the same time, based on the support of graphics processing unit (GPU) acceleration technology and the development of neuromorphic chips, we expect this hardware to advance the BMI technology and improve the effectiveness of the assistive devices. Future work will expand on the relatively simple simulation experiments here and combine the advantages of artificial neural networks and spiking neural networks. For example, SNNs can fully exploit the Spatio-temporal properties of neural information, which is their greatest competitive advantage³⁸. And ANN can effectively explore the hidden structure within the data through data-driven capabilities³⁹. Although in the field of brain-machine interfaces, there has not been a large amount of research on applying brain-inspired intelligence. However, there is growing evidence in neural circuits to support some of these spiking neural network models, and further confirmation of these important experiments is needed. In future applications, a tight combination of neural dynamics and spiking neural networks as well as artificial neural networks, can be used to explore generalized brain-inspired computing architectures based on hybrid models, thus supporting brain-machine interface applications and neuroscience research.

While the work here makes a proof of concept and is preliminary as a first step in applying brain-inspired intelligence to brain-machine interfaces for shared control, making robots with biological control algorithms more functional for future users. This shared approach also balances the user and the automated system, providing high-performance control to the subject while ensuring its accuracy. As brain-machine interface technology and brain-inspired intelligence continue to evolve, these assistive devices will become more accessible and more valuable to those who need them to improve the lives of individuals with impairments.

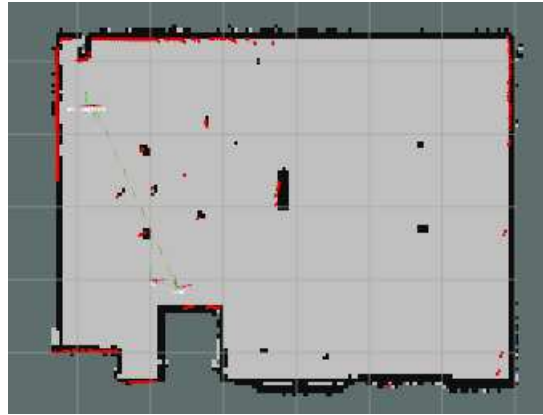


Figure 14. The semantic map generation based on SLAM algorithms

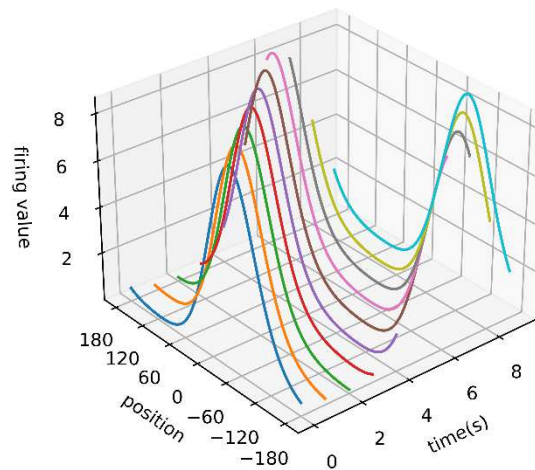


Figure 15. The directional encoding based on the attractor network.

Conclusion

In this paper, collaborative shared control based on brain-inspired intelligence is combined with computer vision to achieve movement control of robotic arms and movement, tracking, and steering of mobile wheeled robots. In real life, robotic control is a complex problem. Invoking brain-inspired intelligence in the system to share some of the work can improve efficiency. The results also suggest that shared control will have great potential for practical applications in brain-machine interfaces. In the future, the collaboration between brain-machine interfaces and brain-inspired intelligence is expected to lead to some real applications to help people with disabilities in their daily lives.

References

1. Collinger, J. L. *et al.* High-performance neuroprosthetic control by an individual with tetraplegia. *The Lancet* **381**, 557–564 (2013).
2. Hochberg, L. R. *et al.* Reach and grasp by people with tetraplegia using a neurally controlled robotic arm. *Nature* **485**, 372–375 (2012).
3. Nuyujukian, P. *et al.* Cortical control of a tablet computer by people with paralysis. *PloS one* **13**, e0204566 (2018).
4. Willett, F. R., Avansino, D. T., Hochberg, L. R., Henderson, J. M. & Shenoy, K. V. High-performance brain-to-text communication via handwriting. *Nature* **593**, 249–254 (2021).
5. Rajeswaran, P. & Orsborn, A. L. Neural interface translates thoughts into type (2021).
6. Simeral, J., Kim, S.-P., Black, M., Donoghue, J. & Hochberg, L. Neural control of cursor trajectory and click by a human with tetraplegia 1000 days after implant of an intracortical microelectrode array. *J. neural engineering* **8**, 025027 (2011).

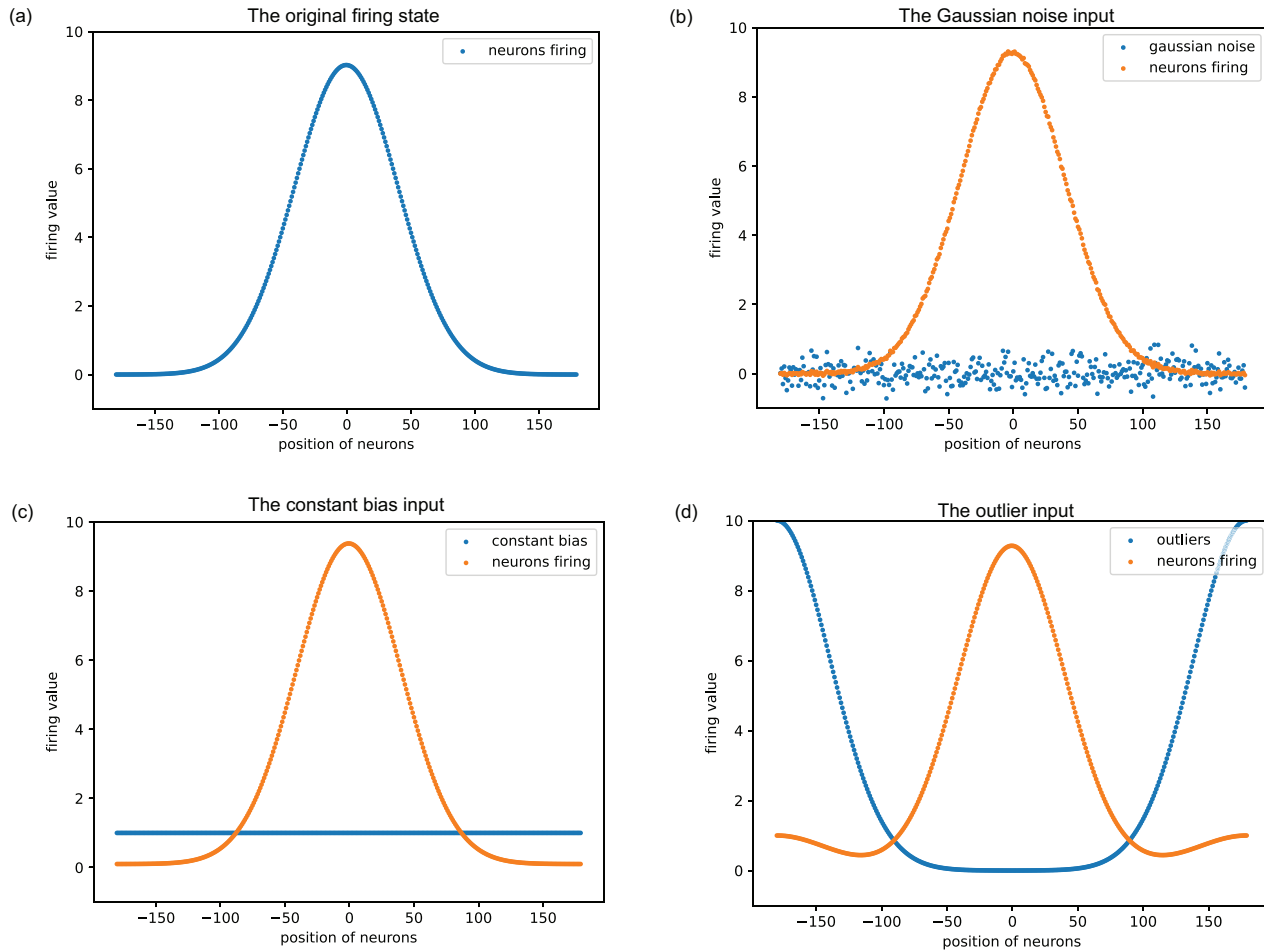


Figure 16. The Gaussian noise, constant bias and outlier input to the original firing state of the continuous attractor as shown in (a), and observe the change of the release state of the attractor network, as shown in (b), (c) and (d).

7. McFarland, D. J., Krusienski, D. J., Sarnacki, W. A. & Wolpaw, J. R. Emulation of computer mouse control with a noninvasive brain–computer interface. *J. neural engineering* **5**, 101 (2008).
8. Pfeifer, R., Lungarella, M. & Iida, F. Self-organization, embodiment, and biologically inspired robotics. *science* **318**, 1088–1093 (2007).
9. Taylor, D. M., Tillery, S. I. H. & Schwartz, A. B. Direct cortical control of 3d neuroprosthetic devices. *Science* (2002).
10. Taylor, D. M., Tillery, S. I. H. & Schwartz, A. B. Direct cortical control of 3d neuroprosthetic devices. *Science* **296**, 1829–1832 (2002).
11. Donoghue, J., Mijail, D., Serruya, G., Hatsopoulos, L. & Matthew, F. Brain-machine interface: Instant neural control of a movement signal. *Nature* **416**, 14 (2002).
12. Chapin, J. K., Moxon, K. A., Markowitz, R. S. & Nicolelis, M. A. Real-time control of a robot arm using simultaneously recorded neurons in the motor cortex. *Nat. neuroscience* **2**, 664–670 (1999).
13. Wessberg, J. *et al.* Real-time prediction of hand trajectory by ensembles of cortical neurons in primates. *Nature* **408**, 361–365 (2000).
14. Carmena, J. M. *et al.* Learning to control a brain–machine interface for reaching and grasping by primates. *PLoS biology* **1**, e42 (2003).
15. Chaudhary, U., Birbaumer, N. & Ramos-Murguialday, A. Brain–computer interfaces for communication and rehabilitation. *Nat. Rev. Neurol.* **12**, 513–525 (2016).

16. Johansson, R. S. & Flanagan, J. R. Coding and use of tactile signals from the fingertips in object manipulation tasks. *Nat. Rev. Neurosci.* **10**, 345–359 (2009).
17. Vogel, J. *et al.* An assistive decision-and-control architecture for force-sensitive hand–arm systems driven by human–machine interfaces. *The Int. J. Robotics Res.* **34**, 763–780 (2015).
18. Katyal, K. D. *et al.* A collaborative bci approach to autonomous control of a prosthetic limb system. In *2014 IEEE International Conference on Systems, Man, and Cybernetics (SMC)*, 1479–1482 (IEEE, 2014).
19. Yonekura, S. & Kuniyoshi, Y. Spike-induced ordering: Stochastic neural spikes provide immediate adaptability to the sensorimotor system. *Proc. Natl. Acad. Sci.* **117**, 12486–12496 (2020).
20. Gallego, J. A., Perich, M. G., Chowdhury, R. H., Solla, S. A. & Miller, L. E. Long-term stability of cortical population dynamics underlying consistent behavior. *Nat. neuroscience* **23**, 260–270 (2020).
21. Chestek, C. A. *et al.* Long-term stability of neural prosthetic control signals from silicon cortical arrays in rhesus macaque motor cortex. *J. neural engineering* **8**, 045005 (2011).
22. Zhang, Z. A flexible new technique for camera calibration. *IEEE Transactions on pattern analysis machine intelligence* **22**, 1330–1334 (2000).
23. Wedderburn, R. W. Quasi-likelihood functions, generalized linear models, and the gauss—newton method. *Biometrika* **61**, 439–447 (1974).
24. DeWolf, T., Stewart, T. C., Slotine, J.-J. & Eliasmith, C. A spiking neural model of adaptive arm control. *Proc. Royal Soc. B: Biol. Sci.* **283**, 20162134 (2016).
25. Voelker, A. R. A solution to the dynamics of the prescribed error sensitivity learning rule. *Centre for Theor. Neuroscience, Waterloo* (2015).
26. Bekolay, T., Kolbeck, C. & Eliasmith, C. Simultaneous unsupervised and supervised learning of cognitive functions in biologically plausible spiking neural networks. In *Proceedings of the Annual Meeting of the Cognitive Science Society*, 35 (2013).
27. Wu, S., Hamaguchi, K. & Amari, S.-i. Dynamics and computation of continuous attractors. *Neural computation* **20**, 994–1025 (2008).
28. Zhang, K. Representation of spatial orientation by the intrinsic dynamics of the head-direction cell ensemble: a theory. *J. Neurosci.* **16**, 2112–2126 (1996).
29. Samsonovich, A. & McNaughton, B. L. Path integration and cognitive mapping in a continuous attractor neural network model. *J. Neurosci.* **17**, 5900–5920 (1997).
30. Kim, S. S., Rouault, H., Druckmann, S. & Jayaraman, V. Ring attractor dynamics in the drosophila central brain. *Science* **356**, 849–853 (2017).
31. Ge, S., Li, J., Ye, Q. & Luo, Z. Detecting masked faces in the wild with lle-cnns. In *Proceedings of the IEEE conference on computer vision and pattern recognition*, 2682–2690 (2017).
32. Bekolay, T. *et al.* Nengo: a python tool for building large-scale functional brain models. *Front. neuroinformatics* **7**, 48 (2014).
33. Quigley, M. *et al.* Ros: an open-source robot operating system. In *ICRA workshop on open source software*, 3.2, 5 (Kobe, Japan, 2009).
34. Handelman, D. A. *et al.* Shared control of bimanual robotic limbs with a brain-machine interface for self-feeding. *Front. Neurobotics* **140** (2022).
35. Dunlap, C. *et al.* Towards a modular brain-machine interface for intelligent vehicle systems control—a carla demonstration. In *2019 IEEE International Conference on Systems, Man and Cybernetics (SMC)*, 277–284 (IEEE, 2019).
36. Downey, J. E. *et al.* Blending of brain-machine interface and vision-guided autonomous robotics improves neuroprosthetic arm performance during grasping. *J. neuroengineering rehabilitation* **13**, 1–12 (2016).
37. Kim, H. K. *et al.* Continuous shared control for stabilizing reaching and grasping with brain-machine interfaces. *IEEE Transactions on Biomed. Eng.* **53**, 1164–1173 (2006).
38. Roy, K., Jaiswal, A. & Panda, P. Towards spike-based machine intelligence with neuromorphic computing. *Nature* **575**, 607–617 (2019).
39. Lillicrap, T. P., Santoro, A., Marris, L., Akerman, C. J. & Hinton, G. Backpropagation and the brain. *Nat. Rev. Neurosci.* **21**, 335–346 (2020).